

# Hi-GMAE: Hierarchical Graph Masked Autoencoders

Chuang Liu\*  
Wuhan University  
chuangliu@whu.edu.cn

Zelin Yao\*  
Wuhan University  
zelinyao@whu.edu.cn

Yibing Zhan  
JD Explore Academy  
zhanyibing@jd.com

Xueqi Ma  
The University of Melbourne  
xueqim@student.unimelb.edu.au

Dapeng Tao  
Yunnan University  
dptao@ynu.edu.cn

Jia Wu  
Macquarie University  
jia.wu@mq.edu.au

Wenbin Hu†  
Wuhan University  
hwb@whu.edu.cn

Shirui Pan  
Griffith University  
s.pan@griffith.edu.au

Bo Du  
Wuhan University  
dubo@whu.edu

## ABSTRACT

Graph Masked Autoencoders (GMAEs) have emerged as a notable self-supervised learning approach for graph-structured data. Existing GMAE models primarily focus on reconstructing node-level information, categorizing them as single-scale GMAEs. This methodology, while effective in certain contexts, tends to overlook the complex hierarchical structures inherent in many real-world graphs. For instance, molecular graphs exhibit a clear hierarchical organization in the form of the *atoms-functional groups-molecules* structure. Hence, the inability of single-scale GMAE models to incorporate these hierarchical relationships often leads to their inadequate capture of crucial high-level graph information, resulting in a noticeable decline in performance. To address this limitation, we propose Hierarchical Graph Masked AutoEncoders (Hi-GMAE), a novel multi-scale GMAE framework designed to handle the hierarchical structures within graphs. First, Hi-GMAE constructs a multi-scale graph hierarchy through graph pooling, enabling the exploration of graph structures across different granularity levels. To ensure masking uniformity of subgraphs across these scales, we propose a novel coarse-to-fine strategy that initiates masking at the coarsest scale and progressively back-projects the mask to the finer scales. Furthermore, we integrate a gradual recovery strategy with the masking process to mitigate the learning challenges posed by completely masked subgraphs. Diverging from the standard graph neural network (GNN) used in GMAE models, Hi-GMAE modifies its encoder and decoder into hierarchical structures. This entails using GNN at the finer scales for detailed local graph analysis and employing a graph transformer at coarser scales to capture global information. Such a design enables Hi-GMAE to effectively capture the multi-level information inherent in complex graph structures. Our experiments on 15 graph datasets,

\*Both authors contributed equally to this work.

†Corresponding Author

Permission to make digital or hard copies of all or part of this work for personal or classroom use is granted without fee provided that copies are not made or distributed for profit or commercial advantage and that copies bear this notice and the full citation on the first page. Copyrights for components of this work owned by others than the author(s) must be honored. Abstracting with credit is permitted. To copy otherwise, or republish, to post on servers or to redistribute to lists, requires prior specific permission and/or a fee. Request permissions from permissions@acm.org.

Conference acronym 'XX, June 03–05, 2018, Woodstock, NY

© 2018 Copyright held by the owner/author(s). Publication rights licensed to ACM.

ACM ISBN 978-1-4503-XXXX-X/18/06

<https://doi.org/XXXXXXXX.XXXXXXX>

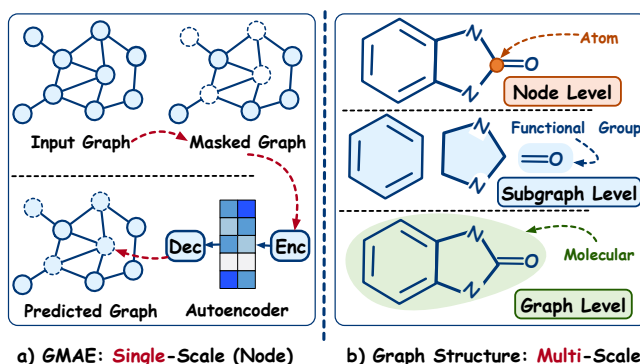


**Figure 1:** a) The GMAE models focus on reconstructing randomly masked nodes using an autoencoder architecture, with a primary focus on the node level, categorizing them as **single-scale** approaches. b) The inherent hierarchical structure of a molecule graph, which contains node, subgraph, and overall graph level information, is termed as **multi-scale**.

covering two distinct graph learning tasks, consistently demonstrate that Hi-GMAE outperforms 17 state-of-the-art self-supervised competitors in capturing comprehensive graph information. Codes are available at <https://github.com/LiuChuang0059/Hi-GMAE>.

## CCS CONCEPTS

- Computing methodologies → Learning latent representations;
- Information systems → Data mining.

## KEYWORDS

Graph Masked Autoencoder, Graph Classification, Self-Supervised Learning, Graph Representation Learning

## ACM Reference Format:

Chuang Liu, Zelin Yao, Yibing Zhan, Xueqi Ma, Dapeng Tao, Jia Wu, Wenbin Hu, Shirui Pan, and Bo Du. 2018. Hi-GMAE: Hierarchical Graph Masked Autoencoders. In *Proceedings of Make sure to enter the correct conference title from your rights confirmation email (Conference acronym 'XX)*. ACM, New York, NY, USA, 15 pages. <https://doi.org/XXXXXXXX.XXXXXXX>

## 1 INTRODUCTION

In many real-world graphs, especially within the academic, social, and biological sectors, the availability of labeled data is often limited. This poses a significant challenge for traditional supervised learning approaches in graph analysis. To address this challenge, Graph Self-supervised Pre-training (GSP) methods have emerged as a powerful tool [2, 14, 19, 25, 34, 43, 57], utilizing the inherent graph data structures and properties to extract meaningful representations without requiring labeled examples. Current GSP methods can be categorized into two primary streams: **1) Contrastive** GSP methods, such as GraphCL [51] and SimGRACE [41], entail constructing multiple graph views through augmentation and learning representations by contrasting positive and negative samples; **2) Generative** GSP methods, such as GraphMAE [11] and MaskGAE [20], emphasize learning node representations through a reconstruction objective. Generative GSP methods have been shown to be simpler and more effective compared to contrastive approaches that require carefully designed augmentation and sampling strategies [10]. Accordingly, this paper explores the capabilities of generative GSP methods, specifically graph masked autoencoders (GMAEs), and further examines their potential in graph learning tasks.

Current GMAE models, as illustrated in Figure 1 (a), primarily focus on reconstructing node features, capturing mainly node-level information. However, this approach type, labeled as **single-scale**, is inconsistent with the **multi-scale** structure inherent in graphs, such as social networks, recommendation networks, and molecular graphs, acknowledged as a cornerstone for graph representation learning [18, 24, 49]. For example, as displayed in the molecular graph in Figure 1 (b), in addition to node-level atom information, a subgraph-level of information exists within functional groups (*i.e.*, benzene rings). This multi-scale nature of the graph enables a richer representation of molecular characteristics, capturing complex interactions and relationships that exceed node-level information. However, current GMAE models face limitations in learning this complex, high-level structural information, resulting in a decline in performance. Therefore, this leads to a question: *how can we effectively capture the hierarchical information inherent in graphs?*

To tackle this challenge, we propose the Hierarchical Graph Masked AutoEncoders (Hi-GMAE). The Hi-GMAE framework comprises three principal components: **1) Multi-scale Coarsening**: The first step in extracting hierarchical information from graphs involves constructing a series of coarse graphs at multiple scales. These scales range from fine- to coarse-grained graphs. Specifically, we utilize graph pooling methods that progressively cluster nodes into super-nodes, thereby generating coarsened graphs. **2) Coarse-to-Fine (CoFi) Masking with Recovery**: Building on the multi-scale coarse graphs, we introduce a novel masking strategy. This strategy is designed to maintain the consistency of masked subgraphs across all scales. The process commences with applying random masking to the coarsest graph. The mask matrix is then back-projected to the finer scales using an unpooling operation. This CoFi approach ensures seamless and consistent masking across various levels of the graph hierarchy. Additionally, to address the challenges of learning from fully masked subgraphs initially, we introduce a gradual recovery strategy, which involves selectively unmasking certain masked nodes. **3) Fine- and Coarse-Grained (Fi-Co) Encoder and Decoder**: To

effectively capture diverse information at different graph scales, we develop a hierarchical encoder that combines both fine-grained graph convolution and coarse-grained graph transformer (GT) modules. The fine-grained graph convolution modules capture local information in low-level graphs, while the coarse-grained GT ones focus on global information in high-level graphs. Correspondingly, a symmetrical and relatively lightweight decoder model is employed. This decoder is tasked with gradually reconstructing and projecting the representations, obtained from the encoder, back to the original graph scale. The hierarchical nature of the encoder and decoder is crucial for comprehensively capturing and representing the multi-level structural information observed in graphs. In summary, Hi-GMAE provides a self-supervised framework for effectively understanding and leveraging hierarchical information in graphs. By integrating multi-scale coarsening, an innovative masking strategy, and a hierarchical encoder-decoder architecture, Hi-GMAE effectively captures the nuances of graph structures at various levels.

To evaluate the effectiveness of the Hi-GMAE model, we conduct comprehensive experiments on a range of widely-used datasets. The experiments include two graph learning tasks: unsupervised and transfer learning. The results demonstrate that Hi-GMAE outperforms existing state-of-the-art models in both contrastive and generative pre-training domains. The improvements highlight the advantages of our multi-scale GMAE approach over conventional single-scale ones. Our main contributions are summarized as follows:

- (1) We introduce Hi-GMAE, a novel self-supervised graph pre-training framework, which incorporates several carefully designed key techniques, including multi-scale coarsening, an innovative masking strategy, and a hierarchical encoder-decoder architecture, to effectively capture multi-scale graph information.
- (2) We evaluate Hi-GMAE’s performance through extensive experiments, comparing its efficacy with generative and contrastive baselines across two graph tasks on various real-world graph datasets. The experimental results consistently validate the effectiveness of Hi-GMAE.

## 2 RELATED WORK

**Graph Self-supervised Pre-training.** Inspired by the success of pre-trained language models, such as BERT [4] and ChatGPT [1], numerous efforts have been directed towards studying GSP. GSP is divided into contrastive and generative methods based on model architecture and objective design. In the past few years, **contrastive** methods have dominated the field of graph representation learning [33, 38, 51, 55]. Its success is largely due to elaborate data augmentation designs, negative sampling, and contrastive loss. In contrast, **generative** methods focus on recovering the missing parts of the input data. For example, GAE [17] is a method that reconstructs the adjacency matrix. Multiple GAE variants utilize graph reconstruction to pre-train Graph Neural Networks (GNNs), including ARVGA [28] and SIGVAE [9]. Recently, a paradigm shift towards GMAEs has displayed promising results in various tasks. GMAEs mainly focus on reconstructing the randomly masked input contents (*e.g.*, nodes and edges) using autoencoder architecture. A prominent and innovative example, GraphMAE [11], reconstructs masked node features, introducing novel techniques such as re-mask decoding and scaled cosine error. In addition, approaches like MaskGAE [20],

S2GAE [35], and GiGaMAE [31] jointly reconstruct masked edges and nodes. Furthermore, the integration of contrastive learning with GMAEs, such as SimSGT [26], HGCVAE [13], and GCMAE [39], and application of self-distillation in RARE [37] further diversify the methodological landscape, enhancing GMAEs' effectiveness. Unlike the above mentioned GMAE methods, which primarily adopt a random masking strategy, StructMAE [22] proposes a novel structure-guided masking strategy. GMAEs are applied across various domains, including heterogeneous graph representation [36], protein surface prediction [52], and action recognition [47]. However, all the aforementioned GMAE methods overlook the hierarchical information inherent in graphs, potentially inhibiting the model's capabilities.

**Hierarchical Graph Learning.** In recent years, hierarchical graph learning has emerged as a pivotal study area within the realm of GNNs. This approach is characterized by its capacity to capture multi-scale structural information, thereby enhancing the effectiveness of learning from graph data. Innovations such as DiffPool [49], Graph U-Nets [7], and SAGPool [18] have been crucial in laying the groundwork for hierarchical representation learning in graphs. These approaches involve strategically reducing graphs into smaller, more condensed subgraphs through pooling, ensuring the preservation of essential structural details. Moreover, further advancements have been achieved with the introduction of hierarchical GT, such as ANS-GT [56] and HSGT [59], thereby scaling and enhancing GT learning. Exploring and applying hierarchical information has also extended to specialized domains, notably the enhancement of molecular [53] and protein [8] representations. These advancements emphasize the potential of hierarchical graph models in handling complex data. Despite this progress, the majority of existing research focuses on supervised learning, with limited attention paid to integrating hierarchical characteristics with GSP, especially concerning generative GSP models. Our work seeks to fully exploit the potential of hierarchical structures in a self-supervised manner.

### 3 PRELIMINARIES

**Notations.** A graph  $\mathcal{G} = (\mathcal{V}, \mathcal{E})$  can be represented by an adjacency matrix  $A \in \{0, 1\}^{n \times n}$  and a node feature matrix  $X \in \mathbb{R}^{n \times d_0}$ , where  $\mathcal{V}$  denotes the node sets,  $\mathcal{E}$  denotes the edge sets,  $n$  is the number of nodes, and  $d_0$  is node feature dimensions. Furthermore,  $A[i, j] = 1$  if an edge between nodes  $v_i$  and  $v_j$  exists; otherwise,  $A[i, j] = 0$ .

**Graph Masked Autoencoders.** GMAEs operate as a self-supervised pre-training framework, which focuses on recovering masked node features or edges based on the unmasked node representations. We explore node feature reconstruction as an illustrative example to elucidate the GMAE methods. GMAEs comprise two essential components: an encoder ( $f_E(\cdot)$ ) and a decoder ( $f_D(\cdot)$ ). The encoder maps each unmasked node  $v_i \in \mathcal{V}_u$  to a  $d$ -dimensional vector  $\mathbf{h}_i \in \mathbb{R}^d$ , with  $\mathcal{V}_u$  representing the unmasked node set, while the decoder reconstructs the masked node features from these vectors. The entire process can be formally represented as:

$$H_u = f_E(A, X_u); \quad \hat{X} = f_D(A, H_u), \quad (1)$$

where  $X_u$  and  $H_u$  denote unmasked nodes' input features and encoded embeddings, respectively, and  $\hat{X}$  represents the reconstructed features of all nodes. In addition, GMAEs optimize the model by minimizing the discrepancy between the reconstructed representation of the masked nodes,  $\hat{X}_m \subset \hat{X}$ , and their original features,  $X_m \subset X$ .

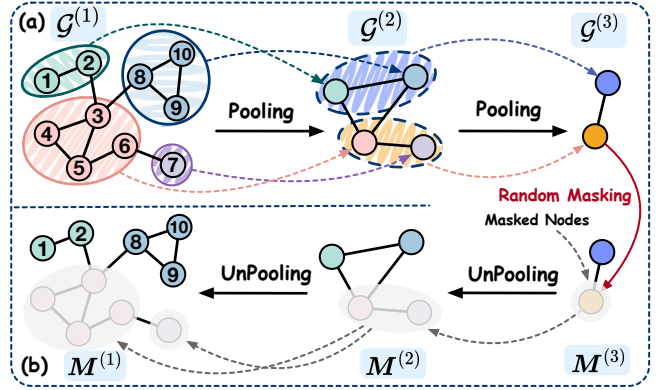


**Figure 2: Illustration of multi-scale graph generation and masking matrix construction. (a) Generating Coarse Graphs:** We utilize the graph pooling algorithm, which clusters nodes into super-nodes, to generate the coarse graph. **(b) CoFi Masking:** We conduct random masking on the coarsest graph and then project the mask matrix onto the fine-grained graph through an unpooling process. This approach ensures that the masking pattern remains consistently aligned across different scales of the graph. Please note that the above two processes, including pooling and unpooling, are iterated across  $S$  scales, although only three scales are presented here for the sake of clarity.

**Graph Pooling and Unpooling.** Graph pooling generates coarse graphs that retain essential information while reducing the number of nodes. This process involves clustering nodes into super-nodes. Given a graph  $\mathcal{G} = (\mathcal{V}, \mathcal{E})$ , the resulting coarse graph is smaller  $\mathcal{G}' = (\mathcal{V}', \mathcal{E}')$ . This is achieved by partitioning  $\mathcal{V}$  into disjoint clusters  $\{C_1, C_2, \dots, C_{n'}\}$ , where each cluster  $C_i$  represents a super-node in the coarse graph  $\mathcal{G}'$ , and  $n' = \|\mathcal{V}'\|$ . The aforementioned pooling process can be further delineated through a cluster assignment matrix  $P \in \{0, 1\}^{n \times n'}$ , where  $P_{ij} = 1$  if node  $v_i$  belongs to cluster  $C_j$ . Then, the new feature and adjacency matrices of  $\mathcal{G}'$  are defined as follows:  $X' = P^T X \in \mathbb{R}^{n' \times d_0}$ , and  $A' = P^T A P \in \mathbb{R}^{n' \times n'}$ . Following the pooling process, the number of nodes in  $\mathcal{G}'$  are significantly reduced compared to  $\mathcal{G}$ . This reduction is quantified by the pooling ratio, defined as  $r_p = n'/n$ . In contrast, the unpooling operations within the encoder-decoder architecture up-sample the coarse representations back to their original resolution. Formally, the unpooling operation can be expressed as:  $X = P X' \in \mathbb{R}^{n \times d_0}$ .

### 4 PROPOSED METHOD

This section describes Hi-GMAE's model architecture. First, we elaborate on the construction of hierarchical graphs (§4.1). Then, we introduce the coarse-to-fine masking module (§4.2). Subsequently, a comprehensive exploration of the fine- and coarse-grained encoder and decoder is provided (§4.3). Additionally, the training and inference details of Hi-GMAE are outlined (§4.4). Finally, the complexity analysis of Hi-GMAE is clarified (§4.5).

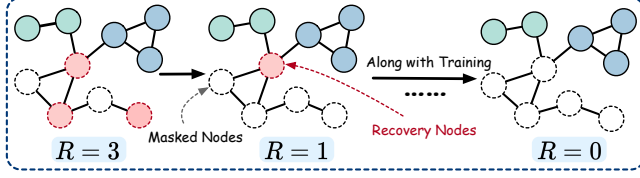


**Figure 3: Illustration of the dynamic node recovery mechanism employed in the CoFi masking. At each epoch, a certain number of nodes are randomly selected for recovery from those that have been masked. The number of recovered nodes (*i.e.*,  $R$ ) gradually decreases along with the training procedure.**

## 4.1 Generating Coarse Graphs

To capture high-level context information within graph structures, our approach involves constructing a series of progressively coarse graphs  $\{\mathcal{G}^{(l)}\}_{l=1}^S$  from the original graph  $\mathcal{G}^{(1)} = \mathcal{G}$ , as illustrated in Figure 2 (a). Each coarse graph  $\mathcal{G}^{(l)}$  represents the graph’s structure at the  $l$ -th coarse level. The depth of this hierarchical structure  $S$  and the pooling ratio  $r_p$  are predefined hyperparameters. Our framework permits flexibility in selecting the graph pooling algorithm, and we opt for METIS [15] due to its efficiency and scalability. This algorithm necessitates only a single computation during the pre-processing phase. The pooling process from the  $(l-1)$ -th scale to the  $l$ -th is mathematically represented as follows:

$$\mathbf{A}^{(l)} = \left(\mathbf{P}^{(l-1)}\right)^\top \mathbf{A}^{(l-1)} \mathbf{P}^{(l-1)} \in \mathbb{R}^{n^{(l)} \times n^{(l)}}, \quad (2)$$

where  $\mathbf{A}^{(l)}$  represents the coarse graph’s adjacency matrix, and  $\mathbf{A}^{(1)} = \mathbf{A}$ . Through iterative pooling, we obtain the  $S$  scale adjacency matrices  $\{\mathbf{A}^{(l)}\}_{l=1}^S$  for the coarse graphs at every hierarchical level.

## 4.2 Coarse-to-Fine Masking with Recovery

**4.2.1 Coarse-to-Fine Masking.** Traditional random masking strategies used in previous GMAE models, while effective in single-scale graphs, fail to ensure the consistency of masked information across multiple scales in hierarchical graph representation learning. To address this challenge, we propose a CoFi masking strategy to manage graph data within the hierarchical encoder, ensuring the consistency of unmasked subgraphs across different scales. Utilizing the coarse graph set  $\{\mathcal{G}^{(l)}\}_{l=1}^S$  generated in §4.1, we first apply random masking to the coarsest graph  $\mathcal{G}^{(S)}$  with a masking matrix  $\mathbf{M}^{(S)} \in \{0, 1\}^{n^{(S)} \times 1}$ , where  $n^{(S)}$  denotes the number of nodes in the  $S$ -th scale. This process generates a new version of the graph where a subset of nodes is masked (*i.e.*, the masked nodes’ features are set to zero). Then, the mask matrix  $\mathbf{M}^{(S)}$  is iteratively back-projected to the lower scales, as depicted in Figure 2 (b). This back-projection is achieved through the unpooling operation, formulated as:

$$\mathbf{M}^{(S-1)} = \left(\mathbf{P}^{(S-1)}\right)^\top \mathbf{M}^{(S)} \in \{0, 1\}^{n^{(S-1)} \times 1}. \quad (3)$$

By applying this recursive back-projection method, we obtain the mask matrix for all the scales in the series, denoted as  $\{\mathbf{M}^{(l)}\}_{l=1}^S$ . This design ensures the consistency of unmasked, visible subgraphs across all the scales.

**4.2.2 The Node Recovery Strategy.** The CoFi masking strategy, while effective in maintaining information consistency across hierarchical graph scales, poses certain challenges. Particularly, initiating masking at the coarsest scale may lead to the masking of entire subgraphs in the original-scale graph (in Figure 2 (b)). This extensive initial masking may hinder the model’s effective reconstruction and learning from these subgraphs, particularly during the early stages of training. To address this issue, we integrate a recovery strategy into the CoFi masking approach. This strategy focuses on selectively unmasking certain nodes within the extensively masked subgraphs, enabling a more gradual and manageable learning process (in Figure 3). Throughout the training process, we systematically reduce the number of nodes being recovered, denoted as  $R^{(l,t)}$ :

$$R^{(l,t)} = n_m^{(l)} \cdot r_{re} \cdot \max\left\{\left(1 - \frac{t}{t_e}\right)^\gamma, 0\right\}, \quad \gamma \geq 0, \quad (4)$$

where  $n_m^{(l)}$  denotes the number of masked nodes at the  $l$ -th scale,  $r_{re}$  denotes the initial recovery ratio (set as 0.5),  $t$  denotes the current epoch,  $t_e$  denotes the end epoch for the recovery operation (set as a quarter of the total epochs), and  $\gamma$  is the decay ratio (set as 1). This gradual decrease serves to progressively intensify the learning difficulty encountered by the models. Hence, the whole recovery strategy can be regarded as a warm-up mechanism for the model’s learning process. By initially presenting the model with a less challenging reconstruction task and gradually increasing the complexity, we experimentally demonstrate that the model can progressively adapt and improve its learning capabilities (see Section 5).

In summary, our approach to learning hierarchical information encompasses a sophisticated process of CoFi masking and recovery (CoFi-R). This comprehensive strategy enables effective learning of graph data at various scales, ensuring that the model progressively adapts and responds to increasing learning challenges.

## 4.3 The Fine- and Coarse-Grained Encoder and Decoder

**4.3.1 The Encoder Process.** Our model employs a multi-scale encoding strategy to process hierarchical graph data (shown in Figure 4), characterized by three distinct stages:

• **Fine-Grained Graph Convolution Encoding:** The graphs with masked features  $\mathbf{H}^{(l)} \in \mathbb{R}^{n^{(l)} \times d}$  are processed by a fine-grained graph convolution encoder, denoted as  $\text{GNN}_{\text{enc}}$  and referred to as GNN in Figure 4. The encoder comprises several GNN layers, such as Graph Isomorphism Networks (GIN) [45]. These layers are designed to capture the local structures present within the masked graph. The process is formulated as below:

$$\mathbf{H}_{\text{enc}}^{(l)} = \text{GNN}_{\text{enc}}^{(l)} \left(\mathbf{A}^{(l)}, \mathbf{H}^{(l)}, \mathbf{M}^{(l)}\right) \in \mathbb{R}^{n^{(l)} \times d}, \quad (5)$$

where  $\mathbf{H}_{\text{enc}}^{(l)}$  denotes the representations at the  $l$ -th coarse scale after the graph convolution,  $n^{(l)}$  denotes the number of nodes in the graph at the  $l$ -th coarse scale, and  $\mathbf{H}^{(1)} = \mathbf{X}$ .

• **Pooling Embeddings:** Following the fine-grained encoding, the output  $\mathbf{H}_{\text{enc}}^{(l)}$  is subjected to a pooling module, denoted as  $\text{POOL}(\cdot)$ . This module functions to project the embeddings to the next level in accordance with the predetermined assignment matrix  $\mathbf{P}^{(l)}$ . As a result of the pooling process, a condensed node embedding matrix

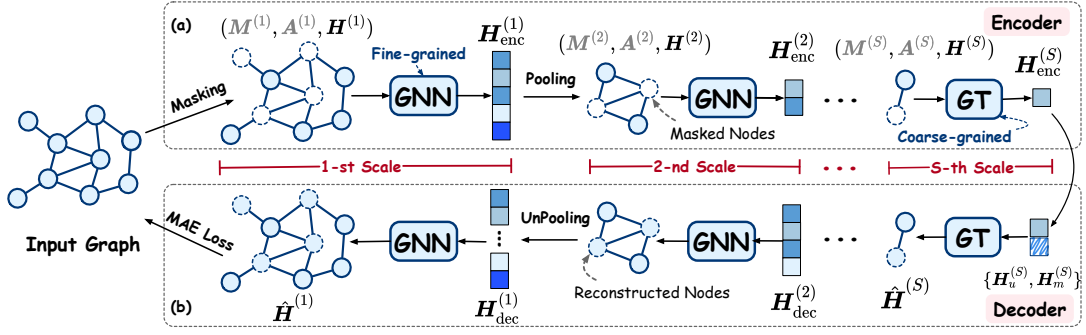


**Figure 4: Overview of the proposed model. (a) Encoder:** The input graph with applied masking first undergoes fine-grained graph convolution (GNN). Following that, the graph undergoes a pooling process. Subsequently, a coarse-grained GT layer (GT) is applied to the coarse graph to facilitate the learning of high-level information. **(b) Decoder:** Upon encoding the unmasked nodes, we employ an unpooling strategy to progressively recover the original graph across different scales. For detailed technical descriptions of masking, pooling, and unpooling, please refer to Section 4.  $(M^{(2)}, A^{(2)})$  in grey signifies that they undergo pre-processing before training.

for the graph at the  $(l + 1)$ -th scale is generated:

$$H^{(l+1)} = \text{POOL} \left( H_{enc}^{(l)} \right) = \left( P^{(l)} \right)^T H_{enc}^{(l)} \in \mathbb{R}^{n^{(l+1)} \times d}. \quad (6)$$

These condense representations present a high-level perspective of the original graph. Please note that we only perform the embedding pooling operations during the pooling stage in Figure 4.

**Coarse-Grained Graph Transformer Encoding:** The coarse graph then becomes the input for the coarse-grained GT [23, 30, 48] encoder. This encoder is tailored to process the graph at a more abstract level, focusing on high-level information and global structures. Only the unmasked nodes in the coarse graphs are transmitted into the self-attention encoder:  $\tilde{H}^{(l+1)} = \{H^{(l+1)}[\text{idx}, :], H_{pe}^{(l+1)}\}$ , where  $\text{idx}$  denotes the index of unmasked nodes, and  $H_{pe}^{(l+1)}$  is the positional encoding derived from the coarse adjacency matrix  $A^{(l+1)}$  through random-walk structural encoding [5]. The encoder process can be succinctly represented using the following formula:

$$H_{enc}^{(l+1)} = \text{Softmax} \left( \frac{\left( \tilde{H}^{(l+1)} W_Q^{(l+1)} \right) \left( \tilde{H}^{(l+1)} W_K^{(l+1)} \right)^T}{\sqrt{d}} \right) \tilde{H}^{(l+1)} W_V^{(l+1)}, \quad (7)$$

where  $H_{enc}^{(l+1)} \in \mathbb{R}^{n_{un}^{(l+1)} \times d}$  denotes the representations of unmasked nodes at the  $(l + 1)$ -th coarse scale after the GT layer.  $W_Q^{(l+1)} \in \mathbb{R}^{d \times d}$ ,  $W_K^{(l+1)} \in \mathbb{R}^{d \times d}$ , and  $W_V^{(l+1)} \in \mathbb{R}^{d \times d}$  are learnable parameters. And,  $n_{un}^{(l+1)}$  denotes the number of unmasked nodes in the  $(l + 1)$ -th scale. Please note that we omit layer normalization and skip connection in Eq. (7) due to space constraints. Then, the output  $H_{enc}^{(l+1)}$  is directed to the next set of pooling and coarse-grained GT encoding layers.

This sequential processing—from fine-grained graph convolutional encoding to pooling embeddings and coarse-grained graph transformer encoding—ensures that our model comprehensively learns the graph at a multi-scale level.

**4.3.2 The Decoder Process.** The decoding mechanism in our model plays a pivotal role in reconstructing the graph structure from its encoded representations. This process involves several key steps.

**Coarse-grained Decoding:** From the hierarchical encoder, we obtain the unmasked nodes' representations at all scales, represented as  $\{H_u^{(l)}\}_{l=1}^S$ , where  $H_u^{(l)} = \hat{H}_{dec}^{(l)}$ . Starting at the coarsest  $S$ -th scale, a shared learnable vector is assigned to each masked node, denoted as  $H_m^{(S)} \in \mathbb{R}^{n_m^{(S)} \times d^{(S)}}$ . Then, these vectors are concatenated with the unmasked node representations, forming a combined representation  $\hat{H}_{dec}^{(S)} = \{H_u^{(S)}, H_m^{(S)}\}$ . This concatenated representation  $\hat{H}_{dec}^{(S)}$  serves as the input for the decoder at the  $S$ -th scale:

$$\hat{H}^{(S)} = f_{dec} \left( A^{(S)}, \hat{H}_{dec}^{(S)} \right) \in \mathbb{R}^{n^{(S)} \times d}, \quad (8)$$

where  $f_{dec}$  represents the decoder network, which is generally lighter than the corresponding encoder network.

**Graph Unpooling to the Finer Scales:** The output  $\hat{H}^{(S)}$  undergoes an unpooling process, denoted as UNPOOL. This unpooling step projects the representations back to the  $(S - 1)$ -th scale:

$$\hat{H}_{dec}^{(S-1)} = \text{UNPOOL} \left( \hat{H}^{(S)} \right) = P^{(S-1)} \hat{H}^{(S)} \in \mathbb{R}^{n^{(S-1)} \times d}. \quad (9)$$

The above two processes are repeated iteratively, scaling from the coarsest scale to the original graph scale. Notably, the decoder choice,  $f_{dec}(\cdot)$ , can vary based on the scale. At the  $S$ -th scale, the decoder can be a GNN or GT layer. However, at other scales, the selected decoder is typically a GNN. This multi-scale approach is critical for capturing and reconstructing the nuanced details and broader structural patterns of the graph.

In summary, integrating the fine-grained graph convolution with coarse-grained graph transformer modules in the encoder and including a symmetrical unpooling process in the decoder define the core functionality of our proposed model. This design facilitates comprehensive and multi-scale learning of the input graph, ensuring that detailed node-level information and broader graph structures are effectively captured and processed.

## 4.4 Training and Inference Details

**Training Process.** The Hi-GMAE training process begins with generating a series of coarse graphs and masking matrices for each hierarchical scale graph. After the coarse graphs and their

respective masking matrices are established, they are processed through Hi-GMAE’s fine- and coarse-grained encoders, yielding the unmasked node representations. The fine-grained encoder focuses on localized node features and structural nuances, while the coarse-grained one emphasizes higher-level graph characteristics, ensuring a comprehensive representation across all the scales. Subsequently, the decoder module reconstructs the masked node features based on unmasked nodes’ representations. To optimize the training process, we adopt the scaled cosine error, as employed in GraphMAE [11].

**Inference for Downstream Tasks.** Hi-GMAE is designed to cater for two distinct downstream applications: unsupervised and transfer learning. During **unsupervised learning**, the encoder processes the input graph without masking in the inference stage. The encoder merges the graph representations across all the scales, effectively capturing the hierarchical essence of the graph structure. For each graph  $\mathcal{G}_i$ , the composite embedding  $\bar{h}_i$  is determined by collecting embeddings  $h_i^{(l)}$  from each scale and applying a readout function:

$$\bar{h}_i = \text{READOUT} \left( \left\{ h_i^{(1)}, h_i^{(2)}, \dots, h_i^{(S)} \right\} \right), \quad (10)$$

where READOUT represents a function (mean, max, sum, or gated operations) designed to merge embeddings from different scales into a singular, comprehensive graph representation. Then, these final embeddings are utilized for graph classification tasks with linear classifiers or support vector machines. In the **transfer learning** context, the pre-trained models are fine-tuned on different datasets. This process mirrors the unsupervised learning approach, where output embeddings are multi-level fused embeddings. This fine-tuning enables the model to adjust to new data domains, leveraging the foundational knowledge gained during its initial training on the source dataset. Both unsupervised and transfer learning applications highlight Hi-GMAE’s flexibility and efficacy in harnessing hierarchical graph structures for comprehensive representation learning.

## 4.5 Complexity Analysis

In this section, we explore the computational complexity of Hi-GMAE, particularly in comparison with GraphMAE [11]. As outlined above, the generation of coarse graphs and the corresponding masks are executed as pre-processing steps. This preliminary processing prepares the graph data for efficient handling in the subsequent stages of the Hi-GMAE model. The primary training distinction between Hi-GMAE and GraphMAE is the inclusion of pooling and unpooling operations. The overall complexity of pooling/unpooling is approximately  $\mathcal{O}(r_p n^2)$  (detailed in the Appendix). Furthermore, the complexity of Hi-GMAE’s coarse-grained encoding module (*i.e.*, self-attention) is quadratic *w.r.t.* the number of input nodes. This complexity exceeds that of traditional GCN-based encoders. However, a crucial optimization within Hi-GMAE ensures that only the coarse graph’s unmasked nodes are processed by the coarse module, thereby adjusting its complexity to  $\mathcal{O}(r_m^2 r_p^2 n^2)$ , where  $r_m$  represents the mask ratio. Notably, when appropriate ratios are selected, so that  $r_p n \ll n$  and  $r_m^2 r_p^2 n \ll n$  (*e.g.*,  $r_m = 0.2$ ,  $r_p = 0.2$ , and  $n = 40$ ), the overall complexity becomes almost linear to  $n$ , making Hi-GMAE a viable and efficient GMAE model.

## 5 EXPERIMENT

### 5.1 Unsupervised Representation Learning

*Objective.* To assess the efficacy of the Hi-GMAE model, we first subject it to the unsupervised learning task, which highlights the model’s feature extraction capabilities. This is necessary because high-quality and informative representations are crucial for various downstream graph tasks.

*Settings. Datasets.* We utilize seven real-world datasets, comprising two in the bioinformatics domain (*i.e.*, PROTEINS and D&D), one in the molecular field (*i.e.*, NCI1), and four in the social sector (*i.e.*, IMDB-B, IMDB-M, COLLAB, and REDDIT-B). **Baseline Models.** To demonstrate our proposed method’s effectiveness, we compare Hi-GMAE with the following 11 baseline models: 1) *Two supervised models*: GIN [45] and DiffPool [49]; 2) *Seven contrastive models*: Infograph [33], GraphCL [51], JOAO [50], GCC [29], InfoGCL [44], SimGRACE [41], and CGKS [54]; 3) *Two generative models*: GraphMAE [11] and S2GAE [35]. **Implementation Details.** In the evaluation phase, encoded graph-level representations, as defined by Eq. (10), are fed into a downstream LIBSVM [3] classifier for graph classification, consistent with other baseline models. We report the mean accuracy across five different runs utilizing a 10-fold cross-validation strategy. Additional details on datasets, baseline models, and hyper-parameter settings are provided in the Appendix.

*Results.* The results are presented in detail in Table 1, where Hi-GMAE-G refers to Hi-GMAE utilizing only GNN as the encoder, and Hi-GMAE-F utilizes the Fi-Co encoder. The following observations can be derived from these results: **1) State-of-the-art Performance.** Hi-GMAE-F outperforms existing self-supervised baselines on six out of the seven datasets. Specifically, Hi-GMAE achieves improvements of 9.8%, 5.6%, and 1.7% in accuracy on the PROTEINS, D&D, and NCI1 datasets, respectively. Furthermore, it achieves state-of-the-art performance considering the average rank across these datasets. In addition, the competitive performance of both Hi-GMAE-F and Hi-GMAE-G emphasizes the importance of incorporating hierarchical information during pre-training, demonstrating the proposed Hi-GMAE approach’s efficacy. **2) Comparison with Supervised Methods.** Remarkably, Hi-GMAE-F, though self-supervised, attains superior performance on six out of the seven datasets compared to supervised methods. This finding indicates that the representations learned by Hi-GMAE-F are high-quality and informative, aligning with the supervised learning benchmarks. **3) Comparison with Generative Methods.** Compared to GraphMAE [11] and S2GAE [35], which are single-scale GMAE models, Hi-GMAE consistently outperforms them across all datasets. This result further supports our hypothesis that leveraging hierarchical structural information can significantly enhance the model’s learning capabilities. **4) The Fi-Co Encoder vs. GNN Encoder.** The superior performance of Hi-GMAE-F over Hi-GMAE-G across almost all the datasets (except for IMDB-B) highlights the advantage of integrating self-attention mechanisms to capture high-level information. The potential reason for the poor performance on the IMDB dataset is its small size, which may lead to the overfitting issue when applying the GT layer. This distinction illustrates the Fi-Co encoder’s ability to capture broader graph information through the GT layer, while GNN encoders primarily focus on local information. These findings

**Table 1: Experimental results for unsupervised representation learning in graph classification. The results for baseline methods are sourced from prior studies. – indicates the absence of corresponding results in the original paper. Bold or underline indicates the best or second-best result, respectively, among self-supervised methods. A.R. denotes the average rank of self-supervised methods.**

		PROTEINS	D&D	NCI1	IMDB-B	IMDB-M	COLLAB	REDDIT-B	A.R.
<i>Supervised</i>	GIN [45]	76.2 $\pm$ 2.8	70.8 $\pm$ 1.1	82.7 $\pm$ 1.7	75.1 $\pm$ 5.1	52.3 $\pm$ 2.8	80.2 $\pm$ 1.9	92.4 $\pm$ 2.5	–
	DiffPool [49]	–	77.6 $\pm$ 0.4	–	72.6 $\pm$ 3.9	–	78.9 $\pm$ 2.3	92.1 $\pm$ 2.6	–
<i>Self-supervised</i>	Infograph [33]	74.44 $\pm$ 0.31	72.85 $\pm$ 1.78	76.20 $\pm$ 1.06	73.03 $\pm$ 0.87	49.69 $\pm$ 0.53	70.65 $\pm$ 1.13	82.50 $\pm$ 1.42	9.5
	GraphCL [51]	74.39 $\pm$ 0.45	78.62 $\pm$ 0.40	77.87 $\pm$ 0.41	71.14 $\pm$ 0.44	48.58 $\pm$ 0.67	71.36 $\pm$ 1.15	89.53 $\pm$ 0.84	8.8
	JOAO [50]	74.55 $\pm$ 0.41	77.32 $\pm$ 0.54	78.07 $\pm$ 0.47	70.21 $\pm$ 3.08	49.20 $\pm$ 0.77	69.50 $\pm$ 0.36	85.29 $\pm$ 1.35	7.0
	GCC [29]	–	–	–	72.0	49.4	78.9	<u>89.8</u>	5.3
	InfoGCL [44]	–	–	80.20 $\pm$ 0.60	75.10 $\pm$ 0.90	51.40 $\pm$ 0.80	80.00 $\pm$ 1.30	–	5.0
	SimGRACE [41]	75.35 $\pm$ 0.09	77.44 $\pm$ 1.11	79.12 $\pm$ 0.44	71.30 $\pm$ 0.77	–	71.72 $\pm$ 0.82	89.51 $\pm$ 0.89	6.0
	CGKS [54]	76.0 $\pm$ 0.2	–	79.1 $\pm$ 0.2	–	–	76.8 $\pm$ 0.1	<b>91.7<math>\pm</math>0.2</b>	4.8
	GraphMAE [11]	75.30 $\pm$ 0.39	78.47 $\pm$ 0.23	80.40 $\pm$ 0.30	75.52 $\pm$ 0.66	51.63 $\pm$ 0.52	80.32 $\pm$ 0.46	88.01 $\pm$ 0.19	4.4
	S2GAE [35]	76.37 $\pm$ 0.43	–	80.80 $\pm$ 0.24	<u>75.76<math>\pm</math>0.62</u>	51.79 $\pm$ 0.36	81.02 $\pm$ 0.53	87.83 $\pm$ 0.27	3.7
	Hi-GMAE-G	<u>76.63<math>\pm</math>0.21</u>	<u>80.03<math>\pm</math>0.45</u>	<u>82.00<math>\pm</math>0.63</u>	<b>76.14<math>\pm</math>0.19</b>	<u>51.93<math>\pm</math>0.37</u>	<u>82.16<math>\pm</math>0.17</u>	88.81 $\pm$ 0.26	<u>2.3</u>
Hi-GMAE-F	<b>83.88<math>\pm</math>0.36</b>	<b>82.83<math>\pm</math>0.66</b>	<b>82.21<math>\pm</math>0.36</b>	75.26 $\pm$ 0.63	<b>52.41<math>\pm</math>0.18</b>	<b>83.60<math>\pm</math>0.84</b>	88.22 $\pm$ 0.41	<b>2.1</b>	

**Table 2: Experimental results for transfer learning on molecular property prediction. The model is initially pre-trained on the ZINC15 dataset and subsequently fine-tuned on the above datasets. The reported metrics are ROC-AUC scores. The results for baseline methods are derived from previous studies. Avg. denotes the average performance.**

	BBBP	Tox21	ToxCast	SIDER	ClinTox	MUV	HIV	BACE	Avg.
No-pretrain(GNN)	70.4 $\pm$ 2.4	74.6 $\pm$ 0.8	63.1 $\pm$ 0.7	58.1 $\pm$ 1.0	64.4 $\pm$ 4.2	71.2 $\pm$ 2.0	76.0 $\pm$ 1.4	77.0 $\pm$ 2.1	69.4
No-pretrain(Fi-Co)	67.9 $\pm$ 2.8	74.1 $\pm$ 1.8	62.2 $\pm$ 1.2	58.3 $\pm$ 1.3	56.4 $\pm$ 5.0	62.1 $\pm$ 2.8	74.1 $\pm$ 1.5	76.6 $\pm$ 3.6	66.5
ContextPred [12]	64.3 $\pm$ 2.8	75.7 $\pm$ 0.7	63.9 $\pm$ 0.6	60.9 $\pm$ 0.6	65.9 $\pm$ 3.8	75.8 $\pm$ 1.7	77.3 $\pm$ 1.0	79.6 $\pm$ 1.2	70.4
AttrMasking [12]	64.3 $\pm$ 2.8	76.7 $\pm$ 0.4	64.2 $\pm$ 0.5	61.0 $\pm$ 0.7	71.8 $\pm$ 4.1	74.7 $\pm$ 1.4	77.2 $\pm$ 1.1	79.3 $\pm$ 1.6	71.1
Infomax [12]	68.8 $\pm$ 0.8	75.3 $\pm$ 0.5	62.7 $\pm$ 0.4	58.4 $\pm$ 0.8	69.9 $\pm$ 3.0	75.3 $\pm$ 2.5	76.0 $\pm$ 0.7	75.9 $\pm$ 1.6	70.3
GraphCL [51]	69.7 $\pm$ 0.7	73.9 $\pm$ 0.7	62.4 $\pm$ 0.6	60.5 $\pm$ 0.9	76.0 $\pm$ 2.7	69.8 $\pm$ 2.7	<b>78.5<math>\pm</math>1.2</b>	75.4 $\pm$ 1.4	70.8
JOAO [50]	70.2 $\pm$ 1.0	75.0 $\pm$ 0.3	62.9 $\pm$ 0.5	60.0 $\pm$ 0.8	81.3 $\pm$ 2.5	71.7 $\pm$ 1.4	76.7 $\pm$ 1.2	77.3 $\pm$ 0.5	71.9
GraphLoG [46]	<b>72.5<math>\pm</math>0.8</b>	75.7 $\pm$ 0.5	63.5 $\pm$ 0.7	61.2 $\pm$ 1.1	76.7 $\pm$ 3.3	76.0 $\pm$ 1.1	77.8 $\pm$ 0.8	<u>83.5<math>\pm</math>1.2</u>	73.4
RGCL [21]	71.2 $\pm$ 0.9	75.3 $\pm$ 0.5	63.1 $\pm$ 0.3	61.2 $\pm$ 0.6	85.0 $\pm$ 0.8	73.1 $\pm$ 1.2	77.3 $\pm$ 0.8	75.7 $\pm$ 1.3	72.7
GraphMAE [11]	72.0 $\pm$ 0.6	75.5 $\pm$ 0.6	64.1 $\pm$ 0.3	60.3 $\pm$ 1.1	82.3 $\pm$ 1.2	76.3 $\pm$ 2.4	77.2 $\pm$ 1.0	83.1 $\pm$ 0.9	73.8
GraphMAE2 [10]	71.6 $\pm$ 1.6	75.9 $\pm$ 0.8	<b>65.6<math>\pm</math>0.7</b>	59.6 $\pm$ 0.6	78.8 $\pm$ 3.0	<u>78.5<math>\pm</math>1.1</u>	76.1 $\pm$ 2.2	81.0 $\pm$ 1.4	73.4
UnifiedMol [58]	70.4 $\pm$ 1.6	75.2 $\pm$ 0.4	63.3 $\pm$ 0.3	62.2 $\pm$ 1.1	81.3 $\pm$ 4.9	76.9 $\pm$ 1.5	77.5 $\pm$ 1.1	80.3 $\pm$ 2.2	73.4
Mole-BERT [42]	71.9 $\pm$ 1.6	<u>76.8<math>\pm</math>0.5</u>	64.3 $\pm$ 0.2	<b>62.8<math>\pm</math>1.1</b>	78.9 $\pm$ 3.0	<b>78.6<math>\pm</math>1.8</b>	78.2 $\pm$ 0.8	80.8 $\pm$ 1.4	74.0
Hi-GMAE-G	<b>72.5<math>\pm</math>1.5</b>	76.3 $\pm$ 0.5	64.5 $\pm$ 0.4	60.5 $\pm$ 0.7	<b>86.4<math>\pm</math>1.0</b>	77.1 $\pm$ 1.8	77.3 $\pm$ 0.9	82.6 $\pm$ 1.0	<u>74.6</u>
Hi-GMAE-F	71.0 $\pm$ 1.1	<b>76.9<math>\pm</math>0.3</b>	<u>65.3<math>\pm</math>0.4</u>	<u>62.0<math>\pm</math>0.7</u>	<u>85.6<math>\pm</math>2.8</u>	77.5 $\pm$ 0.8	<b>78.5<math>\pm</math>0.6</b>	<b>85.0<math>\pm</math>0.6</b>	<b>75.2</b>

collectively affirm the Hi-GMAE method’s core principles and its effectiveness in unsupervised graph representation learning.

## 5.2 Transfer Learning

*Objective.* The objective of assessing Hi-GMAE’s performance in transfer learning task is to evaluate the model’s ability to generalize knowledge acquired during pre-training to unseen datasets.

*Settings. Datasets.* During the initial pre-training phase, Hi-GMAE is trained on a dataset comprising two million unlabeled molecules obtained from the ZINC15 [32] dataset. Subsequently, the

model undergoes fine-tuning on the eight classification benchmark datasets featured in the MoleculeNet dataset [40]. In our evaluation, we adopt a scaffold-split approach for dataset splitting, as outlined in [11]. **Baseline Models.** To demonstrate our proposed method’s effectiveness, we compare Hi-GMAE with the following 12 baseline models: 1) *Three unsupervised models:* Infomax, AttrMasking, and ContextPred [12]; 2) *Four contrastive models:* GraphCL [51], JOAO [50], GraphLOG [46], and RGCL [21]; 3) *Four generative models:* GraphMAE [11], GraphMAE2 [10], UnifiedMol [58], and Mole-BERT [42]. We report the baseline model results from previous papers according to research norms. **Implementation Details.** The

**Table 3: Ablation study of Hi-GMAE components. “w/o Embedding Aggregation” means that only the representation from the first scale is used as the final representation during inference.**

	PROTEINS	D&D	REDDIT-B
<b>Hi-GMAE</b>	<b>83.88<math>\pm</math>0.36</b>	<b>82.83<math>\pm</math>0.66</b>	<b>88.22<math>\pm</math>0.41</b>
w/o Co-Fi Masking	81.44 $\pm$ 0.25	80.64 $\pm$ 0.63	86.50 $\pm$ 1.55
w/o Node Recovery	83.39 $\pm$ 0.34	81.88 $\pm$ 0.41	87.07 $\pm$ 1.94
w/o Embedding Aggregation	82.51 $\pm$ 0.89	81.17 $\pm$ 0.48	79.40 $\pm$ 2.80

experiments are conducted 10 times, and the mean and standard deviation of the ROC-AUC scores are reported. The details regarding datasets, baseline models, and hyper-parameters are comprehensively summarized in the Appendix.

**Results.** The detailed results in Table 2 offer insightful observations into Hi-GMAE’s performance within the transfer learning context. **1) State-of-the-art Performance.** The observed performance improvements with Hi-GMAE, utilizing both GNN and Fi-Co encoders, across a wide range of datasets underscore its efficiency and adaptability. Specifically, Hi-GMAE-F and Hi-GMAE-G achieve a 1.6% and 0.8% improvement in average performance metrics, respectively. Additionally, each method individually achieves top-tier performance on several datasets. These results validate Hi-GMAE’s ability to effectively generalize learned representations across diverse datasets. This makes it a potentially valuable tool for applications where labeled data is scarce or models need to rapidly adapt to new tasks. The results reinforce the significance of hierarchical structure learning in graphs. By capturing multi-scale information, Hi-GMAE can create representations that are more nuanced and informative, which is particularly beneficial for handling complex graph-based tasks. **2) The Superiority of the Fi-Co Encoder.** The results reveal the superior performance of Hi-GMAE-F over Hi-GMAE-G in average metrics and across six out of the eight datasets. This suggests that the Fi-Co encoder’s ability to capture high-level graph information offers a significant advantage over the GNN encoders used in other GMAE methods (e.g., GraphMAE [11] and Mole-BERT [42]), aligning with previous observations in unsupervised learning.

In summary, Hi-GMAE demonstrates notable success across various benchmarks, affirming its competitive performance in unsupervised and transfer learning tasks. This demonstrates the potential of hierarchical and multi-scale approaches to enhance the performance of graph self-supervised learning.

### 5.3 Further Discussions and Analysis

**The Impact of the Hi-GMAE Components.** A detailed study is conducted to evaluate the impact of different components within Hi-GMAE. It is important to note that, except for the components under analysis, all other aspects of the model remain consistent with the comprehensive Hi-GMAE. The results in Table 3 and Figure 5, as outlined below, provide valuable insights into the significance of each component: **1) The CoFi Masking Strategy.** The observed performance reduction in the absence of the CoFi masking strategy (i.e., 2.9% on PROTEINS, 2.6% on D&D, and 1.9% on REDDIT-B) underscores its importance. This strategy

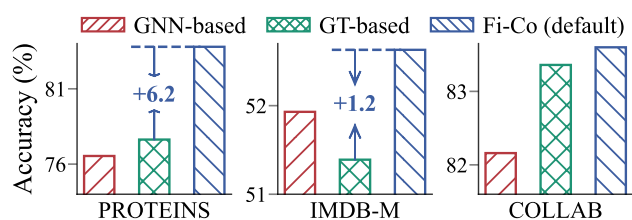


**Figure 5: Comparison of different encoder architectures on three datasets. Fi-Co denotes our proposed fine- and coarse-grained architecture. GNN-based/GT-based characterizes the approach of solely employing GNN/GT as the encoder at every scale.**

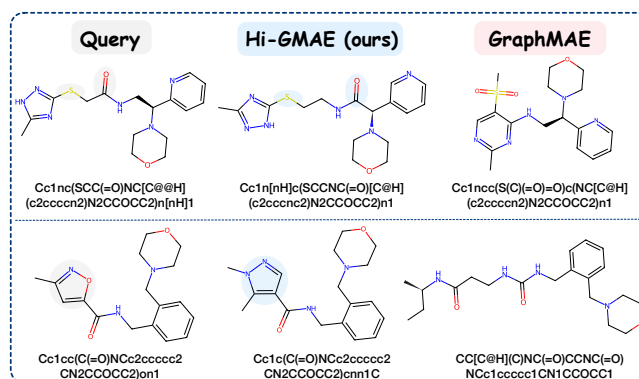


**Figure 6: Visualization of the top-ranked molecule, identified by molecular representation similarity, to the query molecule from ZINC15. The molecule representations obtained from the pre-trained model in the transfer learning task. Further visualization of the top-four molecules is available in the Appendix.**

significantly facilitates capturing the hierarchical graph structure by ensuring the masked information’s consistency across all scales. **2) The Node Recovery.** The positive impact of the node recovery component on Hi-GMAE’s learning process supports the premise that introducing complexity in a phased manner can significantly enhance model learning. This staged complexity approach allows the model to gradually adapt and refine its understanding of the graph’s structure, leading to improved performance. **3) Multi-Scale Representation Aggregation.** Aggregating representations from different scales (refer to Eq. (10)) is especially beneficial for complex datasets like REDDIT-B. This process enables the model to integrate information from various granularity levels, such as from finer details to broader structural patterns, thereby enriching the final graph representation with comprehensive insights. **4) The Fi-Co Encoder.** Compared to the two variants that solely employ GNN or GT architecture as the encoder, our Fi-Co encoder demonstrates superior performance across all the evaluated datasets. This demonstrates that our Fi-Co model is effective at capturing multi-level graph information. In summary, the above findings validate the individual contributions of each component and emphasize their synergy in capturing complex, hierarchical graph data. Due to space constraints, additional parameter analyses are provided in the Appendix.

**The Visualization of Learned Representations.** For a deeper exploration of the semantic information embedded in the pre-trained representations generated by Hi-GMAE (trained on the ZINC15 dataset), we assess the similarity (*i.e.*, cosine similarity) between a given query molecule and other molecules, displaying the top-most similar molecules (more top-four similar molecules are presented in detail in the Appendix). Figure 6 illustrates that the molecule ranked highest by Hi-GMAE (Top@1) exhibits remarkable similarity to the query molecule, mirroring both the types of nodes and the overall graph structure. In contrast, the Top@1 molecule identified by GraphMAE [11] only shares atom types with the query molecule, significantly lacking in replicating essential structural features such as functional groups (*e.g.*, [=O] and SCC). These findings highlight Hi-GMAE’s enhanced capabilities in capturing complex graph structures, indicating its superior efficacy in graph learning tasks.

## 6 CONCLUSION

This study proposes the Hi-GMAE model, a novel multi-scale generative graph pre-training method, featuring several key elements: the generation of multi-level coarse graphs, a CoFi masking strategy with recovery, and a Fi-Co encoder. Through comprehensive experiments covering two distinct graph learning tasks, it is shown that Hi-GMAE excels at capturing hierarchical structural information and significantly outperforms existing self-supervised pre-training methods. These results emphasize the importance of considering the hierarchical structural information inherent in graphs during pre-training. Despite its competitive performance, Hi-GMAE still has room for improvement in several areas, including: 1) improving pooling methods to more effectively exploit hierarchical structural information, and 2) expanding Hi-GMAE’s applicability to a wide range of graph tasks (*e.g.*, node classification and link prediction).

## REFERENCES

- Tom Brown, Benjamin Mann, Nick Ryder, Melanie Subbiah, Jared D Kaplan, Prafulla Dhariwal, Arvind Neelakantan, Pranav Shyam, Girish Sastry, Amanda Askell, et al. 2020. Language models are few-shot learners. In *NeurIPS*.
- Yuxuan Cao, Jiarong Xu, Carl Yang, Jiaan Wang, Yunchao Zhang, Chunping Wang, Lei CHEN, and Yang Yang. 2023. When to Pre-Train Graph Neural Networks? From Data Generation Perspective!. In *SIGKDD*.
- Chih-Chung Chang and Chih-Jen Lin. 2011. LIBSVM: a library for support vector machines. *TIST* (2011).
- Jacob Devlin, Ming-Wei Chang, Kenton Lee, and Kristina Toutanova. 2019. BERT: Pre-training of Deep Bidirectional Transformers for Language Understanding. In *ACL*.
- Vijay Prakash Dwivedi, Anh Tuan Luu, Thomas Laurent, Yoshua Bengio, and Xavier Bresson. 2022. Graph Neural Networks with Learnable Structural and Positional Representations. In *ICLR*.
- Matthias Fey and Jan E. Lenssen. 2019. Fast Graph Representation Learning with PyTorch Geometric. In *ICLR Workshop*.
- Hongyang Gao and Shuiwang Ji. 2019. Graph u-nets. In *ICML*.
- Ziqi Gao, Chenran Jiang, Jiawen Zhang, Xiaosen Jiang, Lanqing Li, Peilin Zhao, Huanming Yang, Yong Huang, and Jia Li. 2023. Hierarchical graph learning for protein–protein interaction. *Nature Communications* (2023).
- Arman Hasanzadeh, Ehsan Hajiramezani, Krishna Narayanan, Nick Duffield, Mingyuan Zhou, and Xiaoning Qian. 2019. Semi-Implicit Graph Variational Auto-Encoders. In *NeurIPS*.
- Zhenyu Hou, Yufei He, Yukuo Cen, Xiao Liu, Yuxiao Dong, Evgeny Kharlamov, and Jie Tang. 2023. GraphMAE2: A Decoding-Enhanced Masked Self-Supervised Graph Learner. In *WWW*.
- Zhenyu Hou, Xiao Liu, Yukuo Cen, Yuxiao Dong, Hongxia Yang, Chunjie Wang, and Jie Tang. 2022. GraphMAE: Self-Supervised Masked Graph Autoencoders. In *SIGKDD*.
- Weihua Hu\*, Bowen Liu\*, Joseph Gomes, Marinka Zitnik, Percy Liang, Vijay Pande, and Jure Leskovec. 2020. Strategies for Pre-training Graph Neural Networks. In *ICLR*.
- Yulan Hu, Zhirui Yang, Sheng Ouyang, and Yong Liu. 2023. HGCVAE: Integrating Generative and Contrastive Learning for Heterogeneous Graph Learning. *arXiv:2310.11102* (2023).
- Xunqiang Jiang, Yuanfu Lu, Yuan Fang, and Chuan Shi. 2021. Contrastive pre-training of GNNs on heterogeneous graphs. In *CIKM*. 803–812.
- George Karypis and Vipin Kumar. 1997. METIS: A software package for partitioning unstructured graphs, partitioning meshes, and computing fill-reducing orderings of sparse matrices. (1997).
- Diederik P Kingma and Jimmy Ba. 2014. Adam: A method for stochastic optimization. *arXiv:1412.6980* (2014).
- Thomas N Kipf and Max Welling. 2016. Variational graph auto-encoders. *arXiv:1611.07308* (2016).
- Junhyun Lee, Inyeop Lee, and Jaewoo Kang. 2019. Self-attention graph pooling. In *ICML*.
- Han Li, Dan Zhao, and Jianyang Zeng. 2022. KPGT: Knowledge-Guided Pre-training of Graph Transformer for Molecular Property Prediction. In *SIGKDD*. 857–867.
- Jintang Li, Ruofan Wu, Wangbin Sun, Liang Chen, Sheng Tian, Liang Zhu, Changhua Meng, Zibin Zheng, and Weiqiang Wang. 2023. What’s Behind the Mask: Understanding Masked Graph Modeling for Graph Autoencoders. In *SIGKDD*.
- Sihang Li, Xiang Wang, An Zhang, Yingxin Wu, Xiangnan He, and Tat-Seng Chua. 2022. Let invariant rationale discovery inspire graph contrastive learning. In *JCLR*.
- Chuang Liu, Yuyao Wang, Yibing Zhan, Xueqi Ma, Dapeng Tao, Jia Wu, and Wenbin Hu. 2024. Where to Mask: Structure-Guided Masking for Graph Masked Autoencoders. In *IJCAI*.
- Chuang Liu, Yibing Zhan, Xueqi Ma, Liang Ding, Dapeng Tao, Jia Wu, and Wenbin Hu. 2023. Gapformer: Graph Transformer with Graph Pooling for Node Classification. In *IJCAI*.
- Chuang Liu, Yibing Zhan, Jia Wu, Chang Li, Bo Du, Wenbin Hu, Tongliang Liu, and Dacheng Tao. 2023. Graph Pooling for Graph Neural Networks: Progress, Challenges, and Opportunities. In *IJCAI*.
- Xiao Liu, Shiyu Zhao, Kai Su, Yukuo Cen, Jiezhong Qiu, Mengdi Zhang, Wei Wu, Yuxiao Dong, and Jie Tang. 2022. Mask and Reason: Pre-Training Knowledge Graph Transformers for Complex Logical Queries. In *SIGKDD*.
- Zhiyuan Liu, Yaorui Shi, An Zhang, Enzhi Zhang, Kenji Kawaguchi, Xiang Wang, and Tat-Seng Chua. 2023. Rethinking Tokenizer and Decoder in Masked Graph Modeling for Molecules. *NeurIPS* (2023).
- Christopher Morris, Nils M Kriege, Franka Bause, Kristian Kersting, Petra Mutzel, and Marion Neumann. 2020. TUDataset: A collection of benchmark datasets for learning with graphs. *arXiv:2007.08663* (2020).
- Shirui Pan, Ruiqi Hu, Guodong Long, Jing Jiang, Lina Yao, and Chengqi Zhang. 2018. Adversarially Regularized Graph Autoencoder for Graph Embedding. In *IJCAI*.
- Jiezhong Qiu, Qibin Chen, Yuxiao Dong, Jing Zhang, Hongxia Yang, Ming Ding, Kuansan Wang, and Jie Tang. 2020. GCC: Graph Contrastive Coding for Graph Neural Network Pre-Training. In *SIGKDD*.
- Ladislav Rampasek, Mikhail Galkin, Vijay Prakash Dwivedi, Anh Tuan Luu, Guy Wolf, and Dominique Beaini. 2022. Recipe for a General, Powerful, Scalable Graph Transformer. In *NeurIPS*.
- Yucheng Shi, Yushun Dong, Qiaoyu Tan, Jundong Li, and Ninghao Liu. 2023. GiGMAE: Generalizable Graph Masked Autoencoder via Collaborative Latent Space Reconstruction. In *CIKM*.
- Teague Sterling and John J Irwin. 2015. ZINC 15–ligand discovery for everyone. *Journal of chemical information and modeling* (2015).
- Fan-Yun Sun, Jordan Hoffman, Vikas Verma, and Jian Tang. 2020. InfoGraph: Unsupervised and Semi-supervised Graph-Level Representation Learning via Mutual Information Maximization. In *ICLR*.
- Mingchen Sun, Kaixiong Zhou, Xin He, Ying Wang, and Xin Wang. 2022. GPPT: Graph Pre-training and Prompt Tuning to Generalize Graph Neural Networks. In *SIGKDD*.
- Qiaoyu Tan, Ninghao Liu, Xiao Huang, Soo-Hyun Choi, Li Li, Rui Chen, and Xia Hu. 2023. S2GAE: Self-Supervised Graph Autoencoders Are Generalizable Learners with Graph Masking. In *WSDM*.
- Yijun Tian, Kaiwen Dong, Chunhui Zhang, Chuxu Zhang, and Nitesh V Chawla. 2023. Heterogeneous graph masked autoencoders. In *AAAI*.
- Wenxuan Tu, Qing Liao, Sihang Zhou, Xin Peng, Chuan Ma, Zhe Liu, Xinwang Liu, Zhiping Cai, and Kunlun He. 2023. RARE: Robust Masked Graph Autoencoder. *IEEE TKDE* (2023).
- Petar Veličković, William Fedus, William L. Hamilton, Pietro Liò, Yoshua Bengio, and R Devon Hjelm. 2019. Deep Graph Infomax. In *ICLR*.
- Yuxiang Wang, Xiao Yan, Chuang Hu, Fangcheng Fu, Wentao Zhang, Hao Wang, Shuo Shang, and Jiawei Jiang. 2023. Generative and Contrastive Paradigms Are Complementary for Graph Self-Supervised Learning. *arXiv:2310.15523* (2023).
- Zhenqin Wu, Bharath Ramsundar, Evan N. Feinberg, Joseph Gomes, Caleb Geniesse, Aneesh S. Pappu, Karl Leswing, and Vijay Pande. 2018. MoleculeNet: a benchmark for molecular machine learning. *Chem. Sci.* (2018).

- [41] Jun Xia, Lirong Wu, Jintao Chen, Bozhen Hu, and Stan Z. Li. 2022. SimGRACE: A Simple Framework for Graph Contrastive Learning without Data Augmentation. In *WWW*.
- [42] Jun Xia, Chengshuai Zhao, Bozhen Hu, Zhangyang Gao, Cheng Tan, Yue Liu, Siyuan Li, and Stan Z. Li. 2023. Mole-BERT: Rethinking Pre-training Graph Neural Networks for Molecules. In *ICLR*.
- [43] Jun Xia, Yanqiao Zhu, Yuanqi Du, and Stan Z. Li. 2022. A survey of pretraining on graphs: Taxonomy, methods, and applications. *arXiv:2202.07893* (2022).
- [44] Dongkuan Xu, Wei Cheng, Dongsheng Luo, Haifeng Chen, and Xiang Zhang. 2021. InfoGCL: Information-Aware Graph Contrastive Learning. In *NeurIPS*.
- [45] Keyulu Xu, Weihua Hu, Jure Leskovec, and Stefanie Jegelka. 2019. How Powerful are Graph Neural Networks?. In *ICLR*.
- [46] Minghao Xu, Hang Wang, Bingbing Ni, Hongyu Guo, and Jian Tang. 2021. Self-supervised graph-level representation learning with local and global structure. In *ICML*.
- [47] Hong Yan, Yang Liu, Yushen Wei, Zhen Li, Guanbin Li, and Liang Lin. 2023. Skeletonmae: graph-based masked autoencoder for skeleton sequence pre-training. In *ICCV*.
- [48] Chengxuan Ying, Tianle Cai, Shengjie Luo, Shuxin Zheng, Guolin Ke, Di He, Yanming Shen, and Tie-Yan Liu. 2021. Do Transformers Really Perform Badly for Graph Representation?. In *NeurIPS*.
- [49] Zhitao Ying, Jiaxuan You, Christopher Morris, Xiang Ren, Will Hamilton, and Jure Leskovec. 2018. Hierarchical Graph Representation Learning with Differentiable Pooling. In *NeurIPS*.
- [50] Yuning You, Tianlong Chen, Yang Shen, and Zhangyang Wang. 2021. Graph contrastive learning automated. In *ICML*.
- [51] Yuning You, Tianlong Chen, Yongduo Sui, Ting Chen, Zhangyang Wang, and Yang Shen. 2020. Graph Contrastive Learning with Augmentations. In *NeurIPS*.
- [52] Mingzhi Yuan, Ao Shen, Kexue Fu, Jiaming Guan, Yingfan Ma, Qin Qiao1, and Manning Wang. 2023. ProteinMAE: Masked Autoencoder for Protein Surface Self-supervised Learning. *Bioinformatics* (2023).
- [53] Xuan Zang, Xianbing Zhao, and Buzhou Tang. 2023. Hierarchical molecular graph self-supervised learning for property prediction. *Communications Chemistry* (2023).
- [54] Yifei Zhang, Yankai Chen, Zixing Song, and Irwin King. 2023. Contrastive Cross-scale Graph Knowledge Synergy. In *SIGKDD*.
- [55] Yifei Zhang, Hao Zhu, Zixing Song, Piotr Koniusz, and Irwin King. 2022. COSTA: Covariance-Preserving Feature Augmentation for Graph Contrastive Learning. In *SIGKDD*.
- [56] Zaixi Zhang, Qi Liu, Qingyong Hu, and Chee-Kong Lee. 2022. Hierarchical Graph Transformer with Adaptive Node Sampling. In *NeurIPS*.
- [57] Ziwen Zhao, Yuhua Li, Yixiong Zou, Jiliang Tang, and Ruixuan Li. 2024. Masked Graph Autoencoder with Non-discrete Bandwidths. In *WWW*.
- [58] Jinhua Zhu, Yingce Xia, Lijun Wu, Shufang Xie, Tao Qin, Wengang Zhou, Houqiang Li, and Tie-Yan Liu. 2022. Unified 2d and 3d pre-training of molecular representations. In *SIGKDD*.
- [59] Wenhao Zhu, Tianyu Wen, Guojie Song, Xiaojun Ma, and Liang Wang. 2023. Hierarchical Transformer for Scalable Graph Learning. In *IJCAI*.

## A PARAMETER ANALYSIS

### A.1 Mask Ratio

In this section, we conduct a detailed analysis to explore how varying mask ratios affect the performance of Hi-GMAE. Upon analyzing the results from Figure 7, it becomes evident that the optimal mask ratio varies depending on the dataset. It is observed that as the mask ratio gradually increases, Hi-GMAE’s accuracy initially improves, which suggests that a certain degree of information omission via masking can indeed enhance learning by forcing the model to better generalize from observed to masked information. However, this trend reverses beyond a certain threshold, where the accuracy gradually decreases as the mask ratio further increases. This suggests that excessive masking may hinder the model’s ability to accurately infer missing information, thereby diminishing its overall performance. Based on our findings, we recommend a mask ratio ranging from 0.4 to 0.6 for deploying Hi-GMAE across various datasets, as this range appears to strike a balance between providing sufficient challenge for effective learning and preserving adequate information for accurate reconstruction and inference.

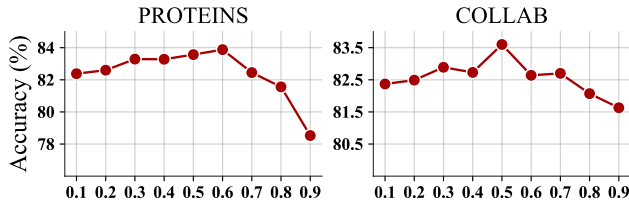


Figure 7: Parameter analysis of the mask ratio.

### A.2 Parameters in Graph Pooling

**Pooling Ratio.** The pooling ratio (i.e.,  $r_p$ ), an important hyperparameter of Hi-GMAE, determines the extent of graph size reduction during the coarsening process. The results illustrated in Figure 8 reveal that: **1)** The PROTEINS dataset exhibits its best performance when the ratio is set to 0.1, while the COLLAB dataset shows optimal results at a pooling ratio of 0.4. As the pooling ratio exceeds its optimal point, there is a gradual decline in performance. **2)** For both PROTEINS and COLLAB datasets, the findings suggest that lower pooling ratios, which imply less aggressive graph reduction, tend to yield better performance. Therefore, in the context of unsupervised tasks, we choose the pooling ratio within the range of 0.1 to 0.5.

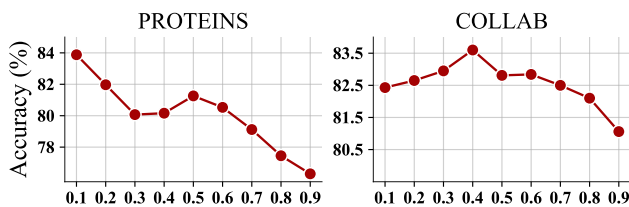


Figure 8: Parameter analysis of the pooling ratio.

**The Number of Pooling Scale.** The varying numbers of scales (i.e.,

S) enable Hi-GMAE to capture diverse hierarchical information in the graph. From the results in Table 4, we can observe that: **1)** The integration of hierarchical information through multiple coarsening layers leads to a marked enhancement in the model’s experimental performance. Specifically, compared to the baseline performance of the single-scale GraphMAE [11], there is a notable increase in performance metrics by 11.39%, 4.08%, and 1.51%. This improvement underscores the value of incorporating multi-scale graph representations to achieve a deeper understanding and more accurate modeling of graph structures. **2)** Across the variety of datasets tested, the optimal configuration for the Hi-GMAE model involves employing between 2 and 3 pooling scales.

Table 4: Impact of the pooling scale.

Dataset	PROTEINS	COLLAB	IMDB-M
GraphMAE	75.30 $\pm$ 0.39	80.32 $\pm$ 0.46	51.63 $\pm$ 0.52
Hi-GMAE (2-scale)	<b>83.88<math>\pm</math>0.36</b>	<b>83.60<math>\pm</math>0.84</b>	50.87 $\pm$ 0.78
Hi-GMAE (3-scale)	76.97 $\pm$ 0.49	81.29 $\pm$ 1.33	<b>52.41<math>\pm</math>0.18</b>
Hi-GMAE (4-scale)	74.48 $\pm$ 1.20	79.44 $\pm$ 2.50	51.53 $\pm$ 0.92

**Pooling Methods.** In our study, we evaluate three graph pooling algorithms (i.e., POOL( $\cdot$ ) in Eq. (6)): Chebyshev, Algebraic JC (JC), and Gauss-Seidel (GS), as implemented by ANS-GT [56]. The results on the PROTEINS, COLLAB, and IMDB-M datasets are shown in Figure 9. This evaluation clearly indicate that the JC method consistently outperforms both the Chebyshev and GS methods across all tested datasets. Specifically, the JC method achieves a performance advantage of 0.46%, 1.44%, and 1.45% over the second-best performing method on the PROTEINS, COLLAB, and IMDB-M datasets, respectively. Given these findings, we have selected the JC method as the default graph pooling approach for Hi-GMAE.

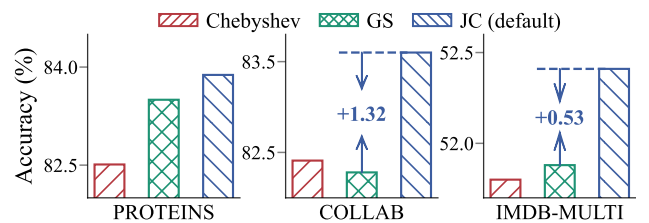
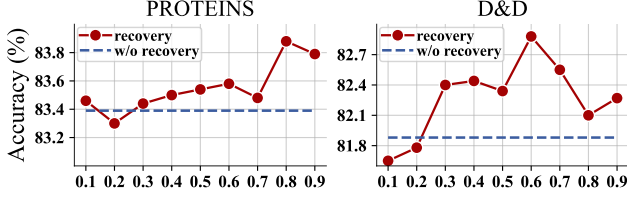


Figure 9: The results of Hi-GMAE with different pooling methods.

### A.3 Parameters in the Node Recovery Strategy

**Recovery Ratio.** The recovery ratio (i.e.,  $r_{re}$  in Eq. (4)) determines the initial restoration proportion in Hi-GMAE. We explore a range of recovery ratios within  $\{0.1, 0.2, \dots, 0.9\}$ . From the detailed statistics in Figure 10, we can infer that: **1)** Utilizing a low recovery ratio results in an insufficient restoration of nodes in the masked subgraphs, which can significantly limit the model’s capability to learn necessary

information from these critical areas. **2)** The CoFi with recovery strategy consistently outperforms the method without recovery across different recovery ratios. This consistency reaffirms our initial finding and underscores the effectiveness of the node recovery strategy in enhancing the model’s accuracy.



**Figure 10: Performance of the CoFi-R strategy with different recovery ratios.**

**Recovery Epoch & Decay Ratio.** For further study the effectiveness of the recovery strategy, we adjust two hyper-parameters in this method. The recovery epoch ratio is explored within the set  $\{0.25, 0.5, 0.75, 1.0\}$ . From Figure 11, the model’s accuracy peaks when the recovery epoch ratio is set to approximately 0.25. This suggests that initiating the recovery process relatively early in the training—specifically, after completing about a quarter of the epochs—provides a beneficial balance between challenge and learning efficiency. Besides, the decay ratio (*i.e.*,  $\gamma$  in Eq. (4)) is searched within  $\{0.25, 0.5, 1, 2, 4\}$ , which includes both linear and non-linear decay options. Figure 11 indicates that a linear decay (*i.e.*,  $\gamma = 1.0$ ) outperforms other configurations. Based on these observations, for the sake of simplicity, we set the recovery epoch ratio as 0.25 and decay ratio as 1.0 in all unsupervised tasks.

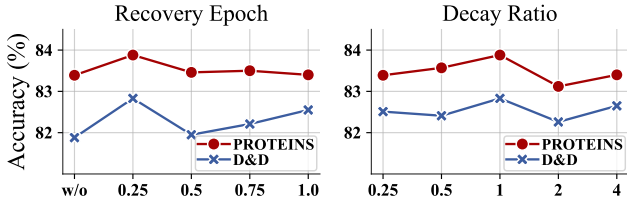


**Figure 11: Performance of the CoFi-R strategy with different recovery epoch and decay ratios.**

## B ABLATION STUDY

### B.1 Hierarchy Reconstruction Loss

In the main text, we introduce a hierarchical graph mask autoencoder to capture hierarchical information within the graph. However, during the computation of loss and graph reconstruction, we only consider the fine-grained graph. In this section, we conduct ablation experiments to assess reconstruction at each hierarchical level. Similar to the implementation approach of U-Net,  $\mathcal{L}_{\text{SCE}}$  is computed on graphs of the same scale and obtained from GraphMAE.

$$\mathcal{L}_{\text{SCE}} = \frac{1}{|\mathcal{V}_m|} \sum_{v_i \in \mathcal{V}_m} \left( 1 - \frac{\mathbf{x}_i^\top \mathbf{h}_i}{\|\mathbf{x}_i\| \cdot \|\mathbf{h}_i\|} \right)^\tau, \tau \geq 1, \quad (11)$$

$$\mathcal{L}_{\text{last}} = \mathcal{L}_{\text{SCE}}(H_m^{(1)}, \hat{H}_m^{(1)}), \quad (12)$$

$$\mathcal{L}_{\text{mid}} = \mathcal{L}_{\text{SCE}}(H_m^{(i)}, \hat{H}_m^{(i)}), i \in (1, S], \quad (13)$$

$$\mathcal{L}_{\text{final}} = \mathcal{L}_{\text{last}} + \alpha * \mathcal{L}_{\text{mid}}, \quad (14)$$

where  $\mathcal{L}_{\text{SCE}}$  represents the loss,  $\mathcal{V}_m$  denotes the masked nodes’ set,  $\mathbf{x}_i$  is the original feature of node  $v_i$ ,  $\mathbf{h}_i \in \hat{H}_m^{(1)}$  is the reconstructed representation of node  $v_i$ , and  $\tau$  is a scaling factor. As shown in the above formula, the final loss ( $\mathcal{L}_{\text{final}}$ ) is computed as the sum of the loss from the finest-grained layer ( $\mathcal{L}_{\text{last}}$ ) and the loss from the intermediate layer ( $\mathcal{L}_{\text{mid}}$ ), multiplied by the coefficient  $\alpha$  (default to 0.5). We conduct experiments on the PROTEINS, COLLAB, and IMDB-M datasets. From the results shown in the Table 5, we find that hierarchical reconstruction accuracy decrease by 0.59%, 2.05%, and 1.08%, respectively.

**Table 5: Ablation of the hierarchy reconstruction loss.**

Method	PROTEINS	COLLAB	IMDB-M
Hierarchy ( $\alpha = 0.5$ )	83.39 $\pm$ 0.39	81.92 $\pm$ 0.20	51.85 $\pm$ 0.66
Finest-grained ( $\alpha = 0$ )	<b>83.88<math>\pm</math>0.46</b>	<b>83.60<math>\pm</math>0.84</b>	<b>52.41<math>\pm</math>0.18</b>

## C COMPLEXITY ANALYSIS

The primary training distinction between Hi-GMAE and GraphMAE is the inclusion of pooling and unpooling operations. At the  $l$ -th scale, Hi-GMAE requires  $\mathcal{O}(r_p^{(l-1)} n \cdot r_p^{(l)} n)$ . With a constant pooling ratio  $r_p$  across all scales, the complexity for all  $S$  scales is simplified to  $\mathcal{O}(r_p n^2 + r_p^3 n^2 + \dots + r_p^{2S-1} n^2)$ . Considering that  $r_p < 1$ ,  $\mathcal{O}(r_p^3 + \dots + r_p^{2S-1})$  is significantly smaller than 1, the overall complexity of pooling/unpooling is approximately  $\mathcal{O}(r_p n^2)$ . Furthermore, the complexity of Hi-GMAE’s coarse-grained encoding module (*i.e.*, self-attention) is quadratic *w.r.t.* the number of input nodes. This complexity exceeds that of traditional GCN-based encoders. However, a crucial optimization within Hi-GMAE ensures that only the coarse graph’s unmasked nodes are processed by the coarse module, thereby adjusting its complexity to  $\mathcal{O}(r_m^2 r_p^2 n^2)$ , where  $r_m$  represents the mask ratio. Notably, when appropriate ratios are selected, so that  $r_p n \ll n$  and  $r_m^2 r_p^2 n \ll n$  (*e.g.*,  $r_m = 0.2$ ,  $r_p = 0.2$ , and  $n = 40$ ), the overall complexity becomes almost linear to  $n$ , making Hi-GMAE a viable and efficient GMAE model.

In addition, Table 6 presents the GPU memory usage and training time for the NCI1 and IMDB-M datasets, comparing HI-GMAE with GraphMAE. Key observations include: **1) Memory Usage:** Hi-GMAE exhibits a slightly memory consumption than GraphMAE. This increased demand is attributed to the use of GT layers as encoders, which are more memory-intensive than GNNs. **2) Time Consumption:** In the pre-processing stage, we coarse each graph to obtain its corresponding coarse-grained adjacency matrix. However, during the training process, Hi-GMAE involves preprocessing multiple graphs in batches, necessitating the aggregation of the coarse-grained adjacency matrices into a unified batch-style adjacency matrix. This aggregation step incurs extra computational overhead and time consumption. We intend to further optimize this aggregation operation in our future work.

**Table 6: Detailed Time & Memory of Hi-GMAE and GraphMAE.**

Method	NCI1		IMDB-M	
	Memory (MB)	Training Time(s)	Memory (MB)	Training Time(s)
GraphMAE	576	1,510.3	608	116.7
Hi-GMAE	682	2,652.6	652	163.8

## D EXPERIMENTAL DETAILS

### D.1 Datasets

**Unsupervised Learning.** For unsupervised representation learning in graph classification, we use seven datasets from TUDataset [27], which vary in content domains and sizes. All the adopted datasets can be downloaded from PyTorch Geometric (PyG) [6].

**Transfer Learning.** For transfer learning on molecular property, we utilized a sample of 2 million unlabeled molecules from the ZINC15 [32] dataset. To evaluate the effectiveness of Hi-GMAE, we fine-tune the model on eight classification datasets from MoleculeNet [40]. The datasets can be accessed from <https://github.com/snap-stanford/pretrain-gnns#dataset-download>. The specific dataset statistics are summarized in Tables 7 and 8.

**Table 7: Statistics of datasets employed in the unsupervised learning task.**

Dataset	# Graphs	# Nodes	# Edges	# Classes	Category
PROTEINS	1,113	39.06	72.82	2	Bioinfo.
D&D	1,178	284.32	715.66	2	
NCI1	4,110	29.87	32.30	2	Molecules
IMDB-B	1,000	19.77	96.53	2	Social Net.
IMDB-M	1,500	13.00	69.54	3	
COLLAB	5,000	74.49	2457.78	3	
REDDIT-B	2,000	429.63	497.75	2	

### D.2 Baseline Models

For the tasks of unsupervised graph classification and transfer learning for molecular property prediction, we leverage existing results from previous studies wherever possible. This approach ensures that our comparisons are grounded in a consistent and fair basis, facilitating a direct evaluation of our model’s performance relative to established benchmarks. Specifically, for the D&D dataset, we explore mask ratios in the set  $\{0.3, 0.4, 0.5\}$  by downloading the source code of GraphMAE and keeping the other settings the same as ours to obtain the results. Furthermore, for the performance evaluation on the IMDB-MULTI dataset, we refer to the results presented by GraphMAE [11] for GraphCL [51] and JOAO [50].

**Table 8: Statistics of datasets employed in the transfer learning task.**

Dataset	Utilization	# Graph	# Nodes	# Edges	# Classes
ZINC	Pre-training	2,000,000	26.62	57.72	–
BBBP	Fine-tuning	2,039	24.06	51.90	1
Tox21	Fine-tuning	7,831	18.57	38.59	12
ToxCast	Fine-tuning	8,576	18.78	38.52	617
SIDER	Fine-tuning	1,427	33.64	70.71	27
ClinTox	Fine-tuning	1,477	26.16	55.77	2
MUV	Fine-tuning	93,087	24.23	52.56	17
HIV	Fine-tuning	41,127	22.5	27.5	1
BACE	Fine-tuning	1,513	34.09	73.72	1

### D.3 Implementation Details of Unsupervised Learning

**Environment.** In unsupervised representation learning, we implement Hi-GMAE with Python (3.11.0), Pytorch (2.1.0), scikit-learn (1.3.1), and Pytorch Geometric (2.4.0). All experiments are conducted on a Linux server with 8 NVIDIA A100 GPUs.

**Parameter Settings.** We use Adam [16] optimizer with  $\beta_1 = 0.9$ ,  $\beta_2 = 0.999$ ,  $\epsilon = 1e - 8$ . Additionally, we use PReLU as our nonlinear activation function. To minimize the introduction of excessive hyper-parameters, we choose to fix the hidden size as 512, coarsening method as JC, recovery epoch as one-quarter of the maximum epoch, and decay ratio as 1.0. For other hyper-parameter selections, we search the coarsening layer in the set  $\{2, 3\}$ , coarse ratio in the set  $\{0.1, 0.2, \dots, 0.5\}$ , and mask ratio in the set  $\{0.1, 0.2, \dots, 0.6\}$ .

**Training Details.** For the pre-training, we use the same encoder type as GraphMAE in the fine-grained layer and GT (i.e., GraphGPS [30]) in the coarse-grained layer. In terms of decoder selection, we also choose the same type of decoder as GraphMAE. At each level, we only utilize a single-layer decoder. For the evaluation, we use a LIBSVM [3] as the classifier with hyper-parameter chosen from  $\{10^{-3}, 10^{-2}, \dots, 1, 10\}$ . We use 10-fold cross validation with 5 different seeds, reporting the average accuracy and variance across five random seeds as the evaluation metrics. The detailed hyper-parameters for reproduction are summarized in Table 9.

**Table 9: Hyper-parameters in unsupervised learning.**

Dataset	PROT.	D&D	NCI1	IM-B	IM-M	COL.	RED-B
Mask ratio	0.6	0.3	0.25	0.3	0.3	0.5	0.6
Encoder	GIN+GT	GIN+GT	GIN+GT	GIN+GT	GIN+GT	GIN+GT	GCN+GT
Decoder	GIN	GIN	GIN	GIN	GIN	GIN	GCN
Num layers	3	1	3	1	1	1	2
Learning rate	0.00015	0.00015	0.0001	0.00015	0.00015	0.00015	0.006
Batch size	32	32	16	32	32	32	8
Pooling layer	2	2	2	3	3	2	3
Pooling ratio	0.1	0.5	0.2	0.3	0.25	0.4	0.2
Recovery ratio	0.8	0.6	0.5	0.0	0.0	0.0	0.7

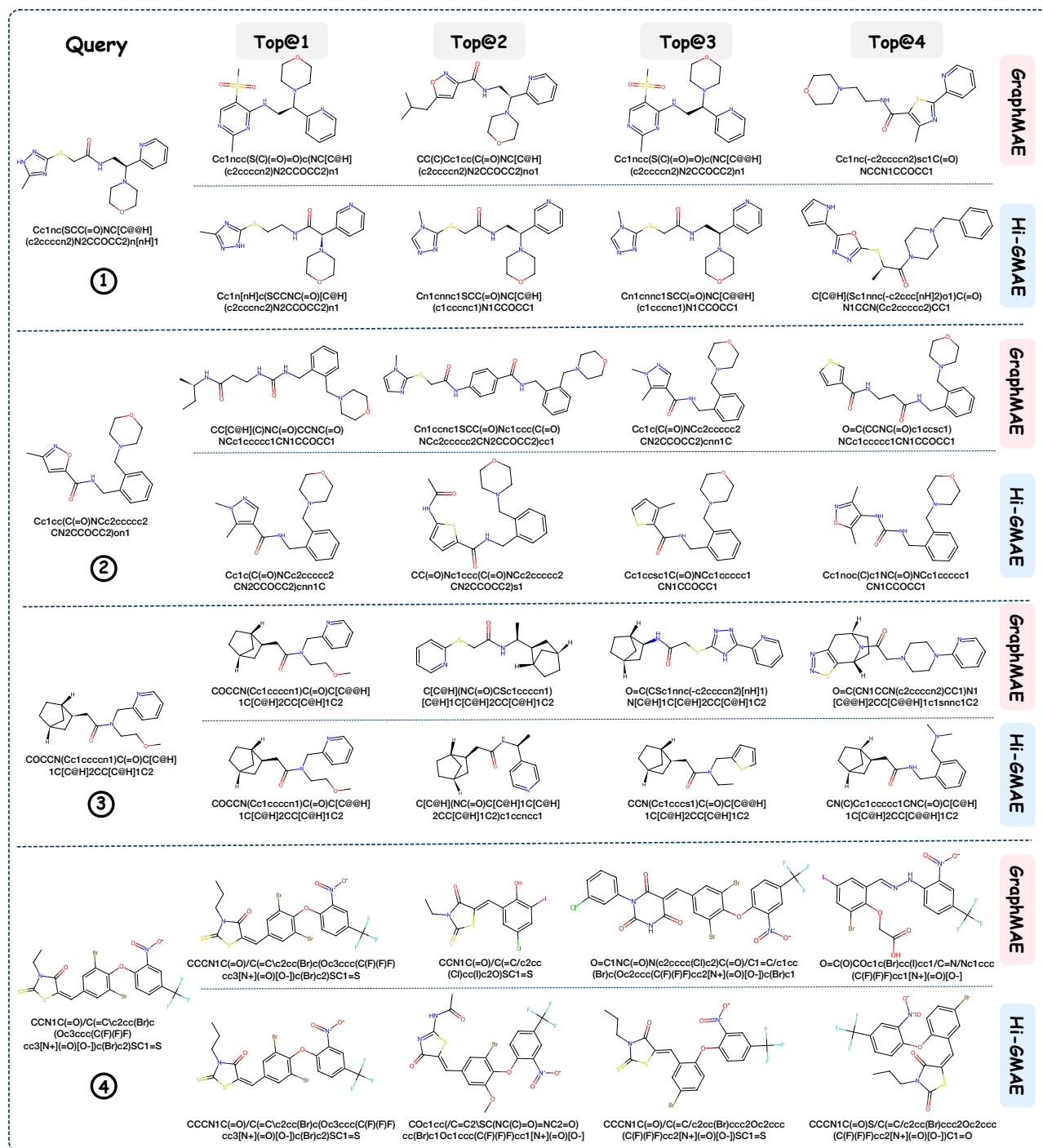


Figure 12: Visualization of the top-four (Top@4) molecule, determined by molecular representation similarity (obtained from the pre-trained model in the transfer learning task), for the query molecule from ZINC15.

#### D.4 Implementation Details of Transfer Learning

**Environment.** In transfer learning, we implement Hi-GMAE with Python (3.9), Pytorch (1.12.0), scikit-learn (1.3.1), rdkit (2022.03.2),

and Pytorch Geometric (2.0.4). All experiments are conducted on a Linux server with 8 NVIDIA A100 GPUs.

**Parameter Settings.** In transfer learning, the CoFi-R strategy is not applied due to the significant time consumption associated with

parameter tuning. For the pre-training, we fix the coarsening layer at 2, mask ratio at 0.25, learning rate at 0.001, batch size at 256, and embedding size at 300. We search the coarsening ratio in the set {0.25, 0.5, 0.75}. For the fine-tuning, we fix the coarsening layer and learning rate the same as pre-training, and dropout ratio at 0.5. Besides, we search the coarsening ratio from 0.1 to 0.9, and batch size in {32, 64}.

**Training Details.** In transfer learning, we adopt a five-layer GIN as the encoder in the fine-grained layer and a single-layer GT in the coarse-grained layer. For the decoder selection, we employ a single GIN layer at each level. We pre-train the model for 100 epochs. For evaluation, the downstream datasets are split into 80/10/10% for train/validation/test using scaffold-split. We report ROC-AUC scores using ten different random seeds. Detailed hyper-parameters of downstream tasks are systematically listed in Table 10.

**Table 10: Hyper-parameters in the fine-tuning phase of transfer learning.**

Dataset	BBBP	Tox21	ToxCast	SIDER	ClinTox	MUV	HIV	BACE
Batch size	32	32	32	32	32	64	32	32
Coarse rate	0.8	0.8	0.8	0.4	0.1	0.6	0.5	0.9

## E VISUALIZATION

In this section, Figure 12 broadens our analysis on molecular similarity, including two examples (*i.e.*, ① and ② in Figure 12) presented in the main text (Figure 6). We can observe that: **1) Structural Information Capturing.** Hi-GMAE successfully captures structural information of molecules, as shown in the first two items of the figure (*i.e.*, ① and ②), while GraphMAE fails to learn structural information starting from Top@1. **2) Consistency in Structure Capturing.** The last two examples (*i.e.*, ③ and ④) illustrate a scenario in which GraphMAE makes an accurate prediction at Top@1, but fails in subsequent predictions, incorrectly identifying the molecular structures. Conversely, Hi-GMAE shows a consistent capability to maintain structural fidelity, closely aligning with the query molecule across its predictions. This consistency demonstrates Hi-GMAE’s advanced proficiency in preserving and predicting the graph structural integrity. **3) Accuracy in Atom Type Prediction.** Hi-GMAE’s proficiency in precisely identifying atom types further underscores its advanced understanding of molecular composition. The incorrect prediction of atom types by GraphMAE, such as the misidentification of bromine (Br) and iodine (I) in ④, highlights the limitations of less sophisticated models. These observations collectively affirm Hi-GMAE’s effectiveness in capturing and representing complex graph structures.

Received 20 February 2007; revised 12 March 2009; accepted 5 June 2009